Technical University of Denmark

DTU

Temperature and field independence of the fluorine and lithium NMR shift tensors in lithium rare-earth tetrafluorides

Nevald, Rolf; Hansen, P. E.

DTU Library
Technical Information Center of Denmark

Temperature and field independence of the fluorine and lithium NMR shift tensors in lithium rare-earth tetrafluorides

R. Nevald and P. E. Hansen*

Department of Electrophysics, The Technical University of Denmark, DK-2800 Lyngby, Denmark
(Received 22 June 1978)

The fluorine and lithium NMR line shifts have been followed in temperature from 300 to 1.3 K and in fields up to 40 kG for $LiTbF_4$ and $LiHoF_4$. The Tb^{3+} and Ho^{3+} ionic moments cause these shifts. The Li shifts are dominated by dipole interactions, whereas the F shifts also have transferred hyperfine contributions of comparable sizes. The transferred hyperfine interactions turn out to be almost isotropic and exhibiting no temperature or field dependence. In $LiHoF_4$ the line shifts are detectable within the entire temperature range. In $LiTbF_4$ the fluorine and lithium lines broaden to such an extent that they disappear in a region from 10 to 60 K and from 15 to 40 K, respectively, probably due to a long relaxation time of the Tb ionic moment.

I. INTRODUCTION

The transferred hyperfine interactions (THI) between the rare-earth ionic moments and the nuclear moments of neighboring diamagnetic ions have been the subject of many investigations, on compounds both dense and dilute in rare-earths. An introduction to the field can be obtained by working backwards through the references of the paper of Reuveni and McGarvey.[1]

We have focused our work on the dense rare-earth trifluorides[2] and lithium rare-earth tetrafluorides.[3] The tetrafluorides are particularly distinguished by simplicity, which makes them attractive for model studies.

The important qualitative questions about the THI's are whether they are strongly anisotropic or predominantly isotropic, whether they are temperature dependent or not, and whether the isotropic parts are positive or negative. In general there seems to be no unique answer, but for the simple systems the THI's are found to be dominantly isotropic, temperature independent, and negative. This was established in the limited temperature region 77–300 K for TbF_3 and DyF_3 in recent work, the limitation being set by NMR line broadening (Hansen *et al.*[2]). Here we report on the results for $LiTbF_4$ and $LiHoF_4$ obtained in the much broader temperature range 1.3–300 K.

II. THEORY

The unit cell of the scheelite structure ($I4_1/a$) contains four formula units, but, as outlined in Ref. 3, they all behave equivalently in a magnetic field applied even in a general direction.

The local magnetic field $\vec{H}_n^{(j)}$ at the jth nucleus of type n (Li or F) is

$$\vec{H}_n^{(j)} = \vec{H}_a + \overleftrightarrow{\sigma}_n^{(j)} \cdot \vec{M}/\rho , \tag{1}$$

where ρ is the density. For a spherical sample in general, the shift tensor $\overleftrightarrow{\sigma}_n^j$ consists of three contributions,

$$\overleftrightarrow{\sigma}_n^{(j)} = \zeta_n \overleftrightarrow{1} + \overleftrightarrow{\epsilon}_n^{(j)} + \overleftrightarrow{\delta}_n^{(j)} , \tag{2}$$

where ζ_n and $\overleftrightarrow{\epsilon}_n^{(j)}$ are the isotropic and anisotropic THI's and $\overleftrightarrow{\delta}_n^{(j)}$ is the point-dipole contributions given by

$$\overleftrightarrow{\delta}_n^{(j)} = \kappa \sum_{\substack{k \text{ in a} \\ \text{sphere}}} \frac{3\vec{r}_{nk}^{(j)}\vec{r}_{nk}^{(j)} - \overleftrightarrow{1}|r_{nk}^{(j)}|^2}{r_{nk}^{(j)5}} , \tag{3}$$

κ being the mass per formula unit and $\vec{r}_{nk}^{(j)}$ the vector from the jth ion of type n to the kth R neighbor.

If one of the fluorine shift tensors (assumed symmetric) in the six-notation is written

$$\overleftrightarrow{\sigma}_F^{(1)} = (\sigma_{Fxx}, \sigma_{Fyy}, \sigma_{Fzz}, \sigma_{Fyz}, \sigma_{Fzx}, \sigma_{Fxy}) , \tag{4}$$

the other three are fixed by symmetry to be

$$\overleftrightarrow{\sigma}_F^{(2)} = (\sigma_{Fyy}, \sigma_{Fxx}, \sigma_{Fzz}, -\sigma_{Fzx}, \sigma_{Fyz}, -\sigma_{Fxy}) ,$$

$$\overleftrightarrow{\sigma}_F^{(3)} = (\sigma_{Fxx}, \sigma_{Fyy}, \sigma_{Fzz}, -\sigma_{Fyz}, -\sigma_{Fzx}, \sigma_{Fxy}) , \tag{5}$$

$$\overleftrightarrow{\sigma}_F^{(4)} = (\sigma_{Fyy}, \sigma_{Fxx}, \sigma_{Fzz}, \sigma_{Fzx}, -\sigma_{Fyz}, -\sigma_{Fxy}) .$$

There is only one lithium shift tensor, and for reasons of symmetry it has the form

$$\overleftrightarrow{\sigma}_{Li} = (\sigma_{Li,xx}, \sigma_{Li,yy}, \sigma_{Li,zz}, 0, 0, 0) . \tag{6}$$

In the experiments presented here the field has always been applied in one of the crystalline axes directions.

This considerably simplifies the following expressions containing only the numerical values of the fields involved, and from the rotational scans presented in Ref. 3 we consider the assignment of the NMR lines as safeguarded.

In the temperature and field ranges where M responds linearly to $\vec{H}_{in} = \vec{H}_a - \frac{4}{3}\pi M$, one finds for the measurable shift $h \equiv (H_n^{(j)2} - H_a^2)/2H_a$, with $\vec{H}_a$ in the

x direction (the crystalline a axis)

$$\frac{h_{F,a}^{(1,3)}}{\chi_\perp(T)H_a} \equiv \frac{(H_F^{(1,3)})^2 - H_a^2}{2\chi_\perp(T)H_a^2}$$

$$= [N_\perp(T)]^{-1}\sigma_{F,xx} + \tfrac{1}{2}\chi_\perp(T)[N_\perp(T)]^{-2}$$

$$\times(\sigma_{F,xx}^2 + \sigma_{F,xy}^2 + \sigma_{F,zx}^2) \;,$$

$$\frac{h_{F,a}^{(2,4)}}{\chi_\perp(T)H_a} \equiv \frac{(H_F^{(2,4)})^2 - H_a^2}{2\chi_\perp(T)H_a^2} \qquad (7)$$

$$= N_\perp(T)^{-1}\sigma_{F,yy} + \tfrac{1}{2}\chi_\perp(T)[N_\perp(T)]^{-2}$$

$$\times(\sigma_{F,yy}^2 + \sigma_{F,yz}^2 + \sigma_{F,xy}^2) \;,$$

and with $\vec{H}_a$ in the z direction (the crystalline c axis)

$$\frac{h_{F,c}^{(1,2,3,4)}}{\chi_{\|}(T)H_a} \equiv \frac{(H_F^{(1,2,3,4)})^2 - H_a^2}{2\chi_{\|}(T)H_a^2}$$

$$= [N_{\|}(T)]^{-1}\sigma_{F,zz} + \tfrac{1}{2}\chi_{\|}(T)[N_{\|}(T)]^{-2}$$

$$\times(\sigma_{F,zz}^2 + \sigma_{F,zx}^2 + \sigma_{F,yz}^2) \;, \qquad (8)$$

$$\frac{h_{Li,c}}{\chi_{\|}(T)H_a} \equiv \frac{(H_{Li})^2 - H_a^2}{2\chi_{\|}(T)H_a^2} = [N_{\|}(T)]^{-1}\sigma_{Li,zz} \;,$$

where $N_\perp(T) = 1 + \tfrac{4}{3}\pi\rho\chi_\perp(T)$ and $N_{\|}(T) = 1 + \tfrac{4}{3}\pi\rho\chi_{\|}(T)$.

Expressions (7) turn out to be usable in the whole temperature and field range, whereas expressions (8) can only be used for $T \gtrsim 20$ K. [It should be noted that the dominant terms in the right-hand side of Eqs. (7) and (8) are those involving the diagonal components of the $\overleftrightarrow{\sigma}_n^{(j)}$ only.]

In the case of nonlinear response of $\vec{M}$ to $\vec{H}$ (i.e., for $T \lesssim 20$ K and H along the c axis) one gets

$$\frac{h_{F,c}^{(1,2,3,4)}}{M_{\|}/\rho} \equiv \frac{(H_F^{(1,2,3,4)})^2 - H_a^2}{2H_a M_{\|}(T,H_a)/\rho}$$

$$= \sigma_{F,zz} + \frac{M_{\|}(T,H_a)/\rho}{2H_a}$$

$$\times(\sigma_{F,zz}^2 + \sigma_{F,zx}^2 + \sigma_{F,yz}^2) \; \qquad (9)$$

and

$$\frac{h_{Li,c}}{M_{\|}/\rho} \equiv \frac{(H_{Li})^2 - H_a^2}{2H_a M_{\|}(T,H_a)/\rho} = \sigma_{Li,zz} \;.$$

The intrinsic susceptibility components $\chi_{\|}(T)$ and $\chi_\perp(T)$ and the magnetization parallel to the c axis $M_{\|}(T,H_a)$ are given in Figs. 1 and 2, respectively, reproduced from the original data of Holmes et al.[4] and Hansen et al.[5]

III. EXPERIMENTAL PROCEDURE

The single crystals were grown from 99.9%-pure materials by the hydrofluorinating method described by Laursen and Holmes.[6] The samples were ground into spheres (3 and 2 mm in diameter for $LiTbF_4$ and $LiHoF_4$, respectively), glued to a copper base with Ge 9031, and oriented in situ
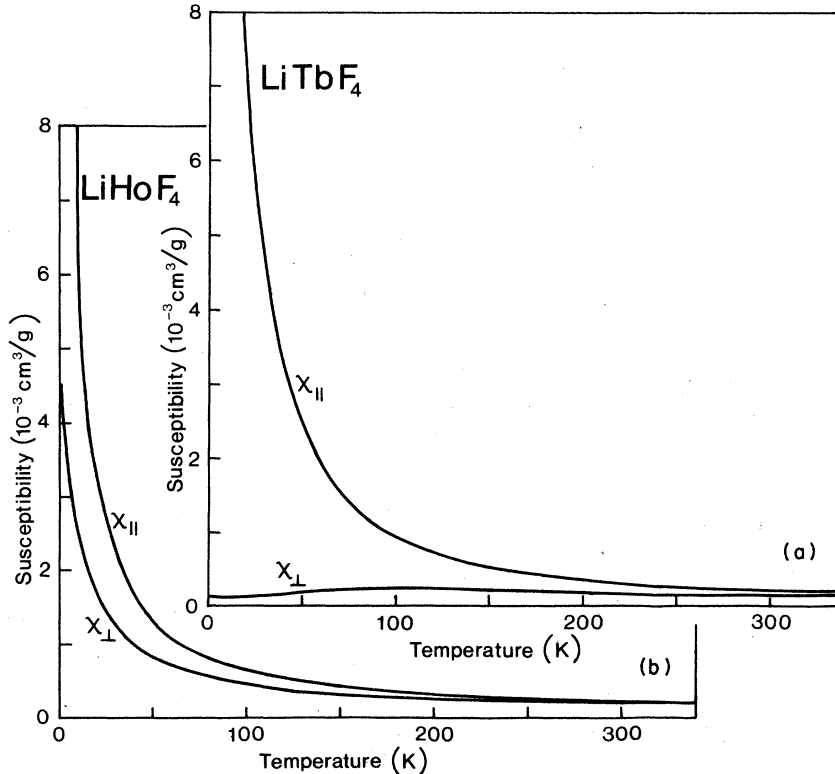

FIG. 1. Intrinsic susceptibility components $\chi_{\|}(T)$ and $\chi_\perp(T)$. (a) $LiTbF_4$ data from Ref. 4. (b). $LiHoF_4$ data from Ref. 5.
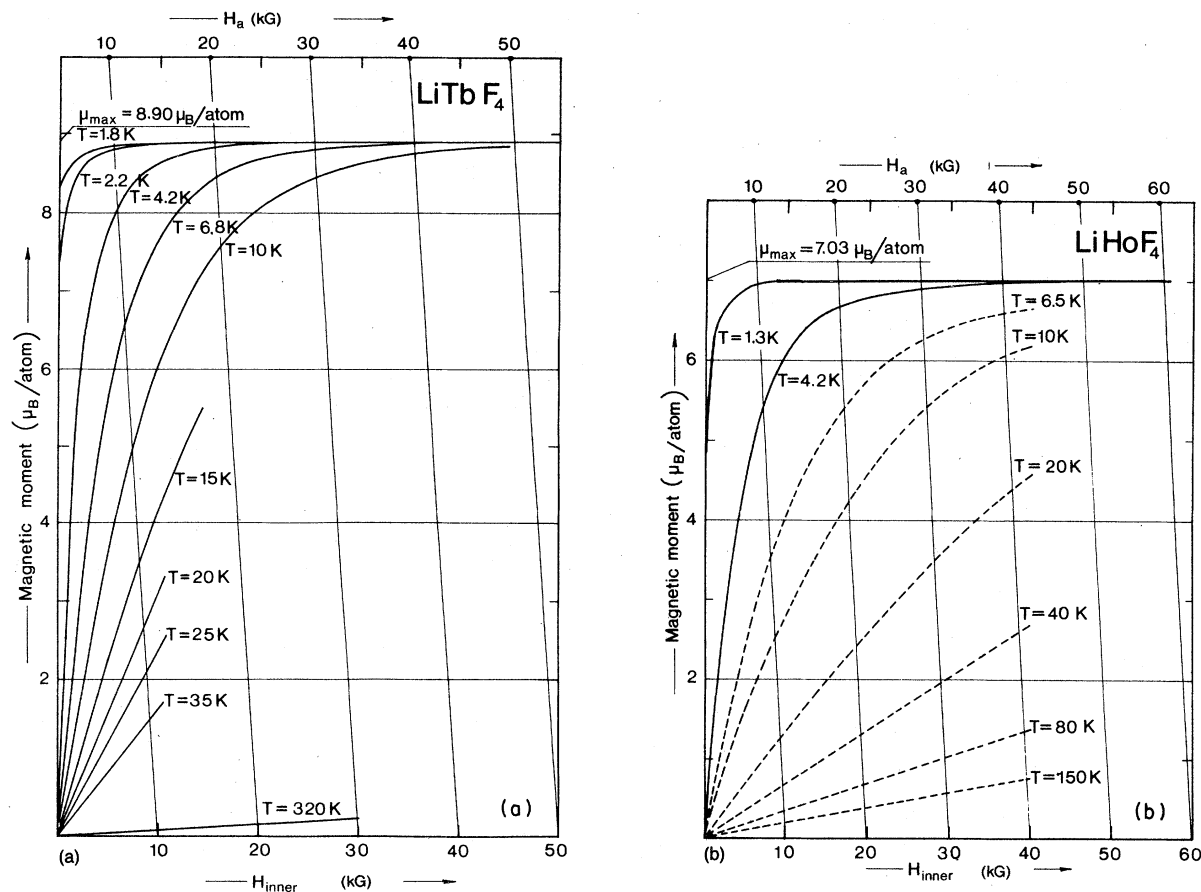
FIG. 2. Magnetization $M_{\parallel}(T, H_a)$ parallel to the c axis at various temperatures and fields. (a). LiTbF$_4$ data from Ref. 4. (b). Experimental LiHoF$_4$ data from Ref. 5 (solid lines), supplemented with calculated data using crystal field parameters from the same reference (dotted lines).

in the NMR sample holder to better than 1°. A self-supporting five-turns coil was placed around the sample and connected to one of several Robinson-type NMR spectrometers through a 55-cm coaxial line. For the high field ^{19}F spectra a special high-frequency NMR spectrometer capable of working up to 300 MHz was used.[7]

All spectra were obtained using field modulation and phase-sensitive detection. The spectrometer frequency was kept fixed and the magnetic field swept through the resonances. The measurements below 77 K, called in the following the low-temperature measurements, were performed in a superconducting magnet, whose field was monitored with an accuracy of ±3 Oe through a precision measurement of the magnet current. (The magnet wire is of the twisted multifilament type, for which current loops are precluded.) The high-temperature measurements, those above 77 K, were taken in an electromagnet, and the field was determined with an NMR gaussmeter, giving an

accuracy of ±50 ppm.

The sample temperatures was obtained from the resistance of an Allen-Bradley carbon resistor below 40 K and of a Cu wire above 40 K. The temperature regulator kept the temperature fixed to better than ±0.5% during a spectral scan. For further details of the setup, Nevald and Hansen[8] may be consulted.

The high-temperature measurements were taken for the magnetic field H_a along the c as well as the a axes. The low-temperature measurements were taken with H_a along the c axis only, because the torque shattered the crystals when H_a was sufficiently strong for NMR measurements and applied along the a axis.

All NMR lines broaden on going down in temperature from 300 K, but whereas for LiHoF$_4$ they stay observable in the whole temperature range, for LiTbF$_4$ the F lines disappear around 60 K and the Li lines at 40 K, probably due to decreasing relaxation rate of the Tb ionic mo-

ment. The F and Li lines reappear for the high-est applied fields at 10 and 15 K, respectively, due to the increasing order in the Tb ionic mo-ments. These observations will be treated in a separate paper.

IV. RESULTS

The ^{7}Li line shifts in $LiTbF_4$ and $LiHoF_4$, $h_{Li}(T, H_a) = (H_{Li}^2 - H_a^2)/2H_a$ measured at various tem-peratures and fields are shown in Table I. The corresponding magnetizations or susceptibilities, needed for the determination of σ_{zz}, are also in-cluded and, finally, the resulting values of σ_{zz}

are quoted. The mean values of σ_{zz} and their standard deviations are extracted and collected in Table IV.

Similarly the ^{19}F line shifts in $LiTbF_4$ and $LiHoF_4$, $h_F^{(j)}(T, H_a) = (H_F^{(j)2} - H_a^2)/2H_a$ are given in Tables II and III, respectively. By the method of least squares, the components of the shift tensors, taken to be temperature and field independent, are determined using Eqs. (7)–(9), and their standard deviations are calculated. (The diagonal and off-diagonal shift components are collected in Tables IV and VI, respectively.) From the fitted shift tensors the two contributions to the mea-sured shifts are calculated and included in Tables

TABLE I. Measured ^{7}Li shifts for various temperatures and fields along the c direction, and the corresponding values of σ_{zz}. For convenience, the magnetization $M_\parallel$ or susceptibility $\chi_\parallel$ (as relevant) is also included.

Temp. (K)	$M_\parallel/\rho$ (Oe cm^3/g) or $\chi_\parallel$ (10^3 cm^3/g)	H_a (Oe)	Shift $\dfrac{H_{Li}^2 - H_a^2}{2H_a}$ (Oe)	σ_{zz} (g/cm^3)
		^{7}Li res. in LiTbF$_4$		
1.3	206	37 741	−1844	−8.95
4.2	205	25 932	−1804	−8.80
4.2	206	33 754	−1822	−8.84
4.2	206	37 896	−1825	−8.86
4.9	206	37 779	−1824	−8.86
5.2	206	33 653	−1825	−8.86
5.7	206	37 777	−1826	−8.87
6.0	205	33 648	−1820	−8.88
7.6	204	37 797	−1823	−8.85
8.0	202	33 608	−1821	−9.00
8.8	202	33 650	−1837	−9.00
10.0	199	33 638	−1810	−9.04
54	2.222	32 380	−613	−9.00
61	2.195	32 289	−525	−9.03
75	1.416	32 142	−405	−9.00
86	1.175	32 082	−326	−8.90
96	0.987	32 028	−269	−8.70
105	0.868	31 988	−235	−8.64
137	0.593	31 925	−160	−8.55
162	0.470	31 891	−125	−8.65
301	0.208	8 310	−16.0	−9.23
		^{7}Li res. in LiHoF$_4$		
4.2	153	26 153	−1515	−9.9
4.2	156	31 004	−1513	−9.7
4.2	157	36 325	−1633	−10.4
12	127	36 100	−1422	−11.2
51	1.316	35 875	−434	−9.2
103	0.641	35 670	−219	−9.6
163	0.402	35 594	−145	−10.1
302	0.204	8 527	−17.4	−10.0

TABLE II. Measured ^{19}F line shifts in LiTbF$_4$, h_F $(T, H_a) = (H_F^2 - H_a^2)/2H_a$ for various temperatures and fields, applied along the crystallographic directions. The shifts are further divided into contribution due to the two parts of the shift tensors, $\sigma_{\alpha\alpha}$ and $\sigma_{\alpha\beta}^2 + \sigma_{\gamma\alpha}^2 + \sigma_{\alpha\alpha}^2$. Also the difference Δ between the measured shifts and the calculated contributions is included.

	Temp. (K)	$M_\parallel/\rho$ (Oe cm^3/g) or $\chi_\parallel$ (10^3 cm^3/g)	H_a (Oe)	Shift $\dfrac{H_F^2 - H_a^2}{2H_a}$ (Oe)	Shift due to $\sigma_{\alpha\alpha}$ (Oe)	Shift due to $\sigma_{\alpha\beta}^2 + \sigma_{\gamma\alpha}^2 + \sigma_{\alpha\alpha}^2$ (Oe)	Δ (Oe)
$\vec{H}_a \parallel \vec{z}$	1.3	206	31 720	-907	-2724	1863	46
$F^{(1, 2, 3, 4)}$	4.2	203	12 083	2105	-2684	4752	-37
$(\alpha = z)$	4.2	203	13 304	1670	-2684	4315	-39
	4.2	204	16 007	921	-2698	3622	3
	4.2	204	16 767	771	-2698	3460	-9
	4.2	205	22 367	-123	-2711	2619	30
	4.2	205	27 245	-586	-2711	2149	24
	4.2	205	29 785	-763	-2711	1966	18
	4.2	205	37 118	-1160	-2711	1578	26
	4.2	205	39 297	-1227	-2711	1490	6
	5.2	205	27 827	-615	-2711	2104	7
	5.5	205	27 798	-640	-2711	2106	35
	5.6	205	27 851	-634	-2711	2102	25
	6.0	205	27 827	-622	-2711	2108	18
	6.0	205	27 798	-639	-2711	2101	29
	6.0	205	27 799	-633	-2711	2106	28
	6.5	204	27 786	-622	-2708	2086	0
	6.5	204	27 755	-610	-2698	2089	1
	6.5	204	27 840	-631	-2699	2082	14
	7.0	203	27 770	-609	-2686	2068	-9
	7.0	203	27 749	-606	-2686	2070	-10
	7.0	203	27 836	-625	-2686	2063	2
	7.3	203	27 764	-605	-2686	2069	-12
	7.6	202	27 750	-605	-2672	2050	-17
	7.6	202	27 840	-631	-2673	2042	1
	7.9	202	37 509	-1177	-2672	1514	19
	8.0	202	27 780	-621	-2673	2047	-5
	8.5	201	27 820	-612	-2659	2024	-23
	9.0	200	27 806	-596	-2646	2005	-44
	60.0	2.024	36 994	-712	-948	211	-24
	72.0	1.501	36 837	-615	-707	116	-23
	89.0	1.103	36 669	-453	-522	62	-7
	101	0.919	8 157	-93.3	-99.3	9.6	3.6
	113	0.781	36 554	-330	-369	31	-7
	128	0.658	32 590	-255	-280	20	-5
	142	0.562	32 559	-212	-239	14	-13
	161	0.476	32 541	-183	-203	10	-10
	171	0.436	8 149	-45.5	-46.4	2.2	1.2
	201	0.351	8 147	-36.8	-37.5	1.4	0.7
	308	0.202	8 042	-20.8	-21.5	0.5	-0.1
$\vec{H}_a \parallel \vec{x}$	80	0.235	8 069.2	-13.8	-14.6	1.0	0.2
$F^{(2, 4)}$	97	0.241	8 074.5	-13.7	-15.0	1.1	-0.2
$(\alpha = y)$	126	0.230	8 081.8	-13.0	-14.3	1.1	-0.2
	163	0.206	8 060.8	-12.0	-12.8	0.8	0
	205	0.180	8 052.9	-11.2	-11.2	0.6	0.6
	253	0.155	8 040.5	-8.9	-9.6	0.5	-0.3
	304	0.135	8 037.3	-8.0	-8.4	0.4	0

TABLE II. (*Continued*)

	Temp. (K)	$M_{\parallel}/\rho$ (Oe cm³/g) or $\chi_{\parallel}$ (10³ cm³/g)	H_a (Oe)	Shift $\dfrac{H_F^2 - H_a^2}{2H_a}$ (Oe)	Shift due to $\sigma_{\alpha\alpha}$ (Oe)	Shift due to $\sigma_{\alpha\beta}^2 + \sigma_{\gamma\alpha}^2 + \sigma_{\alpha\alpha}^2$ (Oe)	Δ (Oe)
$\vec{H}_a \parallel \vec{x}$	80	0.235	8 121.3	-66.5	-67.9	1.0	-0.4
$F^{(1,3)}$	97	0.241	8 128.9	-68.2	-69.7	1.0	-0.5
$(\alpha = x)$	126	0.230	8 135.3	-65.9	-66.6	1.0	0.3
	163	0.206	8 106.4	-59.2	-59.5	0.8	0.9
	205	0.180	8 094.1	-52.2	-52.0	0.6	0.8
	253	0.155	8 074.5	-44.1	-44.6	0.4	-0.1
	304	0.135	8 068.2	-38.6	-38.9	0.3	0

TABLE III. Measured ^{19}F shifts in LiHoF$_4$, $h_F\,(T, H_a) = (H_F^2 - H_a^2)/2H_a$, for various temperatures and fields applied along the crystallographic axes. The shifts are divided into contributions due to the two parts of the shift tensors, $\sigma_{\alpha\alpha}$ and $\sigma_{\alpha\beta}^2 + \sigma_{\gamma\alpha}^2 + \sigma_{\alpha\alpha}^2$. Also the difference Δ between the measured shifts and the calculated contributions is included.

	Temp. (K)	$M_{\parallel}/\rho$ (Oe cm³/g) or $\chi_{\parallel}$ (10³ cm³/g)	H_a (Oe)	Shift $\dfrac{H_F^2 - H_a^2}{2H_a}$ (Oe)	Shift due to $\sigma_{\alpha\alpha}$ (Oe)	Shift due to $\sigma_{\alpha\beta}^2 + \sigma_{\gamma\alpha}^2 + \sigma_{\alpha\alpha}^2$ (Oe)	Δ (Oe)
$\vec{H}_a \parallel \vec{z}$	4.2	152	22 111	1457	-902	2401	42
$F^{(1,2,3,4)}$	4.2	155	27 690	1093	-919	1994	-18
$\alpha = z$	4.2	157	35 642	702	-931	1589	-44
	38	1.786	36 559	-116	-371	247	-8
	52	1.290	36 571	-127	-271	132	-12
	65	1.020	36 594	-147	-216	83	14
	85	0.770	8 339.5	-27.7	-37.4	11.0	1.2
	110	0.592	8 297.1	-22.7	-28.7	6.5	0.5
	140	0.462	8 289.5	-18.1	-22.5	4.0	-0.3
	160	0.402	8 271.0	-16.6	-19.5	3.0	0.0
	185	0.344	8 261.5	-14.7	-16.7	2.2	0.2
	210	0.302	8 266.4	-12.8	-14.7	1.7	-0.2
	240	0.262	8 298.3	-11.4	-12.8	1.3	-0.1
$\vec{H}_a \parallel \vec{x}$	85	0.534	8 304.8	7.5	3.6	4.3	0.4
$F^{(2,4)}$	110	0.426	8 224.4	6.4	2.9	2.7	-0.8
$\alpha = y$	140	0.344	8 266.1	3.6	2.3	1.8	0.5
	160	0.304	8 283.2	3.1	2.1	1.4	0.4
	185	0.268	8 256.2	3.5	1.8	1.1	-0.6
	210	0.240	8 247.7	2.4	1.6	0.9	0.1
	240	0.212	8 321.3	2.1	1.5	0.7	0.0
$\vec{H}_a \parallel \vec{x}$	85	0.534	8 436.6	-142.1	-143.4	0.6	-0.8
$F^{(1,3)}$	110	0.426	8 327.1	-113.1	-113.3	0.4	0.2
$\alpha = x$	140	0.344	8 381.0	-93.1	-92.3	0.2	1.1
	160	0.304	8 348.6	-82.2	-81.3	0.2	1.0
	185	0.268	8 332.2	-71.8	-71.6	0.1	0.3
	210	0.240	8 310.0	-63.5	-64.0	0.1	-0.4
	240	0.212	8 386.2	-56.3	-57.1	0.1	-0.7

TABLE IV. Shift tensor diagonal components and the isotropic THI for ^{7}Li and ^{19}F in LiTbF$_4$ and LiHoF$_4$ in g/cm^3.

| | LiTbF$_4$ | | LiHoF$_4$ | |
	^{19}F	^{7}Li	^{19}F	^{7}Li
σ_{xx}	-35.81 ± 0.82	4.4 ± 1[a]	-32.26 ± 0.40	5.0 ± 1[a]
σ_{yy}	-7.75 ± 0.46	4.4 ± 1[a]	0.81 ± 0.24	5.0 ± 1[a]
σ_{zz}	-13.20 ± 0.12	-8.88 ± 0.18	-6.00 ± 0.09	-10.0 ± 0.6
ζ	-18.92 ± 0.94	0 ± 1	-12.48 ± 0.48	0 ± 1

[a]From Ref. 3 (295 K data)

II and III. Finally, the difference between the sum of the two calculated shift contributions and the measured shifts are given.

To give a further impression of the experimental material, the shifts are plotted for LiTbF$_4$ with H_a applied along the c axis in Fig. 3. To the left the shifts are shown at 4.2 K for varied field, and to the right the shifts are given at 33 kG for varied temperature. For higher temperatures, where the shifts get relatively small, they are also drawn in a fourfold expanded scale. The top figure presents the ^{7}Li shifts, whereas the bottom figure shows the ^{19}F shifts. For ^{19}F the two contributions from different parts of the shift tensors are also plotted. It can be seen that although the shifts and the relative magnitudes of the two contributions vary strongly, the fitting can be done without resorting to temperature- or field-dependent shift tensors.

We have chosen to present the experimental material rather extensively to demonstrate that at least for these crystals the temperature and field dependence of the shift tensors are indeed negligible.

V. DISCUSSION

In our earlier paper on NMR in lithium rare-earth tetrafluorides[3] all the components of the shift tensors at room temperature were measured. Thereby it was found that the isotropic THI with the F nuclei was negative and comparable in size to the dipole tensor components, whereas

the anisotropic THI was less than 10% of the dipole tensor and probably down in the experimental noise.

In this paper we have chosen to follow closely some selected tensor components through a large temperature region and up to 40 kG in applied field. These are primarily the diagonal components σ_{xx}, σ_{yy}, and σ_{zz} and, to a lesser degree, $\sigma_{zx}^2 + \sigma_{yz}^2$, which appear in Eqs. (8) and (9). [$\sigma_{xy}^2 + \sigma_{zx}^2$ and $\sigma_{yz}^2 + \sigma_{xy}^2$ enter Eqs. (7) with so little weight that the experiments render them very inaccurate]. It has to be mentioned that although the shifts increase up to 100 times on cooling to low temperature, the linewidth increases, too, from ~6 G at room temperature through very large values around 30 K to ~50 G at liquid-He temperatures. This means that the accuracy of the determination of the shift tensor components rises at most a factor of 10 on expanding the temperature region. Still, this means an improvement on the accuracy of σ_{xx}, σ_{yy}, and σ_{zz}.

The most important fact, however, learned from the present measurements—as can be seen from Tables I–III—is that inside the experimental accuracy, σ_{xx}, σ_{yy}, σ_{zz}, and $\sigma_{zx}^2 + \sigma_{yz}^2$ are temperature independent between 1.3 and 300 K, and field independent up to 40 kG.

Also the soundness of the basic expression (1) for the local field seems rather convincingly demonstrated, considering the very different conditions at 300 K, where the magnetic ions are slightly polarized only, and at 4.2 K, where they are nearly saturated. Furthermore, at room tem-

TABLE V. Diagonal components of the anisotropic THI tensor for ^{7}Li and ^{19}F in LiTbF$_4$ and LiHoF$_4$ in g/cm^3. All components are zero inside the experimental accuracy.

| | LiTbF$_4$ | | LiHoF$_4$ | |
	^{19}F	^{7}Li	^{19}F	^{7}Li
ϵ_{xx}	1.2 ± 2.2	-0.4 ± 1	-0.7 ± 2.0	0.0 ± 1
ϵ_{yy}	-0.8 ± 2.0	-0.4 ± 1	0.6 ± 2.0	0.0 ± 1
ϵ_{zz}	-0.4 ± 2.0	0.8 ± 1	0.1 ± 2.0	0.0 ± 1

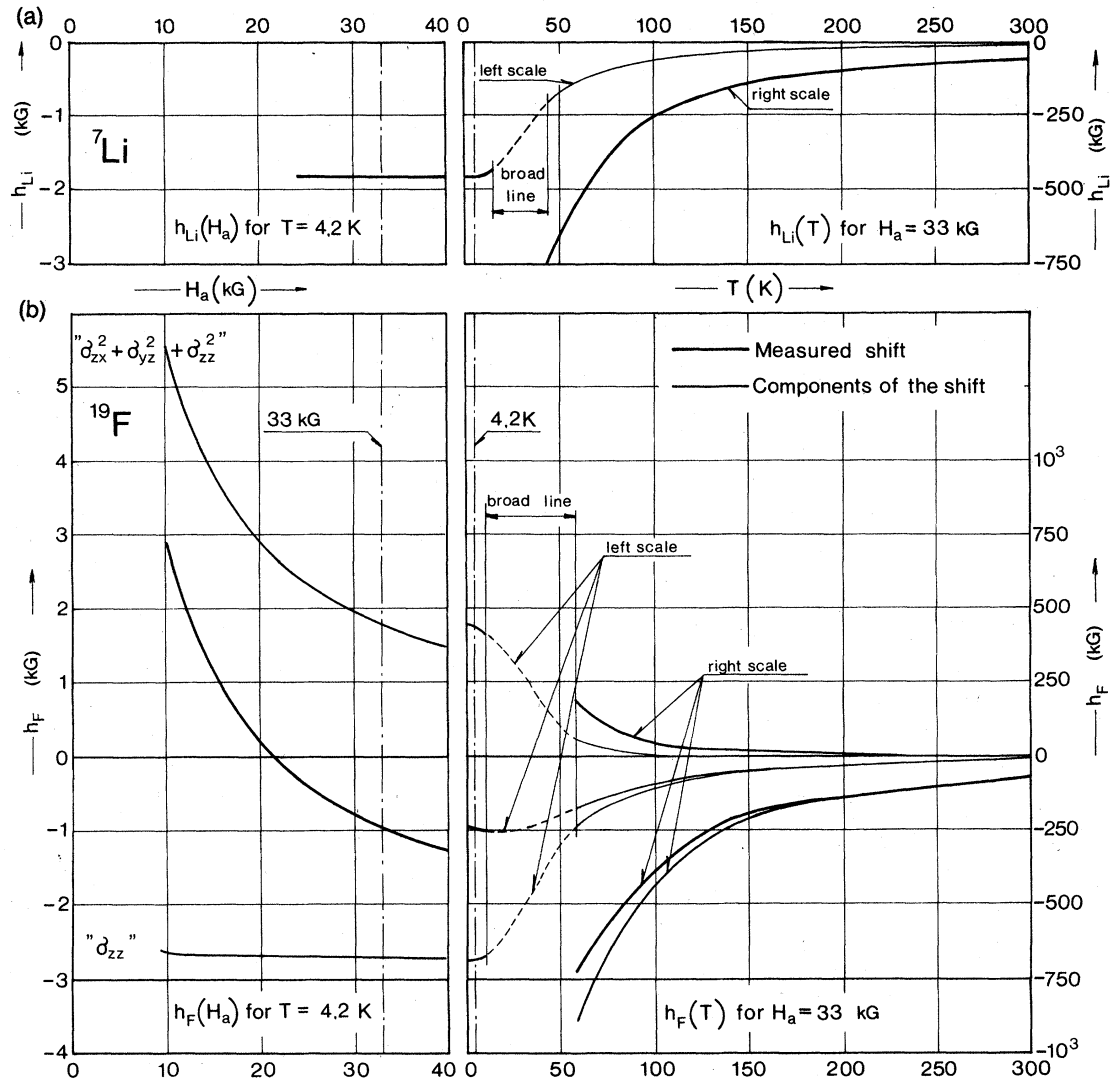FIG. 3. Measured line shifts in LiTbF$_4$ with H_a along the c axis for various fields and temperatures. (a). ^{7}Li line shifts. (b). ^{19}F line shifts. Their divisions in shifts due to $\sigma_{F,zz}$ and $(\sigma^2_{F,zz}+ \sigma^2_{F,zx}+ \sigma^2_{F,yz})$ are also shown.

TABLE VI. Shift tensor off-diagonal components for ^{19}F in LiTbF$_4$ and LiHoF$_4$ compared to those calculated from Ref. 3 and from the dipole tensor. (All values in g/cm^3.) The uncertainty of ± 3 g/cm^3 on the dipole tensor combinations is due to lack of knowledge of the exact fluorine positions.

^{19}F $\alpha\beta\gamma$	LiTbF$_4$ $(\sigma^2_{\alpha\beta} + \sigma^2_{\gamma\alpha})^{1/2}$ This work	Ref. 3	$(\delta^2_{\alpha\beta} + \delta^2_{\gamma\alpha})^{1/2}$	LiHoF$_4$ $(\sigma^2_{\alpha\beta} + \sigma^2_{\gamma\alpha})^{1/2}$ This work	Ref. 3	$(\delta^2_{\alpha\beta} + \delta^2_{\gamma\alpha})^{1/2}$
xyz	(48 ± 40)	23 ± 1	23 ± 3	(0 ± 50)	24 ± 1	25 ± 3
yzx	(60 ± 50)	53 ± 1	57 ± 3	(61 ± 12)	61 ± 1	60 ± 3
zxy	52.0 ± 0.5	52 ± 1	56 ± 3	66 ± 1	63 ± 1	60 ± 3

perature all levels of the magnetic ion are sig-
nificantly populated, whereas at liquid-He tem-
peratures only the lowest level contributes to the
magnetization.

From σ_{nxx}, σ_{nyy}, and σ_{nzz}, the isotropic THI's ζ_n
$= \frac{1}{3}(\sigma_{nxx} + \sigma_{nyy} + \sigma_{nzz})$ can be determined, and they are
included in Table IV.

ζ_F is negative for both LiTbF$_4$ and LiHoF$_4$, and
the absolute value is smallest for LiHoF$_4$, which
has the smallest f-shell radius. (The present
value of ζ_F for LiHoF$_4$ is different from the earlier
reported value from the 295-K data[3] considering
the claimed accuracy. As the larger amount of
experimental data in the present work has allowed
us to calculate the accuracy, we believe the esti-
mated accuracy in the earlier work to be too op-
timistic.)

ζ_{Li} is found to be zero for both materials. This
was to be expected, the Li ions being electropos-
itive and far away from the magnetic ions.

In this paper we are primarily focusing on the
diagonal components of the shift tensors. In or-
der to determine whether there are nonzero an-
isotropic THI diagonal components, the isotropic
THI and the dipole tensor diagonal components
(calculated in Ref. 3) are subtracted from the cor-
responding components of the measured shift ten-
sors. The results for both Li and F sites are
presented in Table V. It is seen that all aniso-
tropic THI components are zero inside the exper-
imental accuracy.

The off-diagonal components of the shift tensors
are only of secondary interest in this work. Still,
the measured combinations as well as those found
at 295 K (Ref. 3) are compared (Table VI) to the
corresponding combinations of the dipole tensor
components. Only the zx and yz combinations are
well determined in this study. Their values,
which we have shown to hold in the whole tempera-
ture region 1.3–300 K, are near to those found at
295 K in Ref. 3 and to the pure dipole contribu-
tions. These agreements, together with the near
coincidence of the individual off-diagonal compo-
nents of the shift and dipole tensors in Ref. 3,
strongly suggest that the whole shift tensor is in-
deed temperature (and field) independent, and that
the anisotropic THI is at least an order of mag-

nitude smaller than the dipole interaction and the
isotropic THI.

According to the spectroscopic work of Chris-
tensen,[9] small structural changes occur in LiTbF$_4$
between 1.3 and 300 K, while this is not seen in
LiHoF$_4$.[10] These changes in LiTbF$_4$ influence the
NMR line shifts both via the crystal-field-depen-
dent susceptibility and through alterations in the
shift tensors. Only the latter mechanism would
show up in the results, since we use the measured
susceptibility in the data treatment. As the re-
sults for LiTbF$_4$ as well as for LiHoF$_4$ lead to
temperature-independent shift tensors, the changes
observed by Christensen for LiTbF$_4$ are conse-
quently too small to influence the shift tensor sig-
nificantly.

VI. CONCLUSION

In the lithium rare-earth tetrafluorides, the iso-
tropic THI between the rare-earth ionic moment
and the F nucleus is temperature independent from
liquid-He temperature to room temperature, and
field independent up to 40 kG. We have found the
same temperature independence to be valid in
rare-earth trifluorides, but in the narrower tem-
perature region 77–300 K.

The fluoride isotropic THI is found to be nega-
tive, and the absolute value to decrease on going
to heavier rare earths. The anisotropic THI is
much smaller. These features are also in qual-
itative agreement with our findings for the tri-
fluorides. The isotropic as well as the anisotropic
THI between the rare-earth ionic moment and the
Li nuclei is negligibly small.

*Present address: HG-ER, L21, V9, Danfoss, DK-6430
Nordborg, Als, Denmark.
[1]A. Reuveni and B. R. McGarvey, J. Magn. Reson. 29, 21
(1978).
[2]P. E. Hansen, R. Nevald, and H. G. Guggenheim, Phys.
Rev. B 17, 2866 (1978).
[3]P. E. Hansen and R. Nevald, Phys. Rev. B 16, 146
(1977).
[4]L. M. Holmes, T. Johansson, and H. J. Guggenheim,

Solid State Commun. 12, 993 (1973).
[5]P. E. Hansen, T. Johansson, and R. Nevald, Phys. Rev.
B 12, 5315 (1975).
[6]I. Laursen and L. M. Holmes, J. Phys. C 7, 3765 (1974).
[7]J. O. Rahbek (unpublished).
[8]R. Nevald and P. E. Hansen, Rev. Sci. Instrum. 49,
64 (1978).
[9]H. P. Christensen, Phys. Rev. B 17, 4060 (1978).
[10]H. P. Christensen (private communication).